

Synthesis and X-ray crystal structures of $[\text{Ru}_4\text{H}_4(\text{CO})_{11}(\text{PPh}_3)]$ and $[\text{Ru}_{4-x}\text{Ir}_x\text{H}_{2-x}(\text{CO})_{12}(\text{PPh}_3)]$ ($x = 0$ or 1)

Aapo U. Härkönen^a, Markku Ahlgrén^a, Tapani A. Pakkanen^{a,*}, Jouni Pursiainen^b

^a Department of Chemistry, University of Joensuu, P.O. Box 111, FIN-80101 Joensuu, Finland

^b Department of Chemistry, University of Oulu, Linnanmaa, FIN-90571 Oulu, Finland

Received 5 June 1996; revised 30 July 1996

Abstract

Three tetranuclear clusters $[\text{Ru}_4\text{H}_4(\text{CO})_{11}(\text{PPh}_3)]$ (**1**), $[\text{Ru}_4\text{H}_2(\text{CO})_{12}(\text{PPh}_3)]$ (**2**) and $[\text{Ru}_3\text{IrH}(\text{CO})_{12}(\text{PPh}_3)]$ (**3**) were formed in the reaction of $[\text{Ir}(\text{CO})\text{Cl}(\text{PPh}_3)_2]$ and $\text{Na}[\text{Ru}_3\text{H}(\text{CO})_{11}]$ in tetrahydrofuran. Complexes **1–3** were characterized by IR and ^1H and ^{31}P NMR, and the structure of the clusters was confirmed by single crystal X-ray analysis. In **2** and **3** one of the carbonyls bridges between two ruthenium atoms; otherwise the compounds contain only terminal carbonyls.

Keywords: Ruthenium; Cluster; Crystal structure; Iridium; Carbonyl

1. Introduction

The chemistry of tetranuclear ruthenium cluster compounds has been extensively investigated during the last 30 years. The preparation of $[\text{Ru}_4\text{H}_4(\text{CO})_{12}]$ was first reported in 1966 [1,2] and its triphenylphosphine and trimethylphosphite mono-substituted derivatives were published in 1971 [3,4]. The mono-substituted PPh_3 derivative has been characterized spectroscopically [3], but there is no report of the crystal structure. However, the corresponding crystal structure of $[\text{Ru}_4\text{H}_4(\text{CO})_{11}\{\text{P}(\text{OMe})_3\}]$ [5] is known and the structures of $[\text{Ru}_4\text{H}_4(\text{CO})_{12}]$ [1,2,6,7] and $[\text{Ru}_4\text{H}_4(\text{CO})_{10}(\text{PPh}_3)_2]$ [3,7,8] have been determined by X-ray diffraction.

The tetranuclear ruthenium cluster $[\text{Ru}_4\text{H}_2(\text{CO})_{13}]$ was synthesized in 1968 [6,9], and later its structure was characterized crystallographically [10]. Tetranuclear ruthenium clusters are also known for two anionic structures: $[\text{Ru}_4\text{H}(\text{CO})_{13}]^-$ [11] and $[\text{Ru}_4\text{H}_2(\text{CO})_{12}]^{2-}$ [12]. The first of these has been characterized crystallographically.

In this work, $[\text{Ir}(\text{CO})\text{Cl}(\text{PPh}_3)_2]$ was allowed to react with $\text{Na}[\text{Ru}_3\text{H}(\text{CO})_{11}]$ in THF. Two tetranuclear Ru clusters, $[\text{Ru}_4\text{H}_4(\text{CO})_{11}(\text{PPh}_3)]$ (**1**) and $[\text{Ru}_4\text{H}_2(\text{CO})_{12}(\text{PPh}_3)]$ (**2**), and some mixed-metal tetranuclear clusters were formed. The ruthenium clusters were characterized

by X-ray crystallography, and by ^1H and ^{31}P NMR and IR spectroscopy. The structure of **2** contains a bridging carbonyl ligand.

2. Results and discussion

The reactions of $[\text{Ir}(\text{CO})\text{Cl}(\text{PPh}_3)_2]$ and $\text{Na}[\text{Ru}_3\text{H}(\text{CO})_{11}]$ in different solvents produce complex mixtures of Ru–Ir mixed-metal clusters and Ru_4 clusters. Characterization of the mixed-metal species is in progress [13]. In the present paper we describe only the reaction and products in THF, where the Ru_4 species were most abundant.

2.1. Spectroscopic data and solid state structure of $[\text{Ru}_4\text{H}_4(\text{CO})_{11}(\text{PPh}_3)]$ (**1**)

The crystal structure of **1** is shown in Fig. 1. With minor variations, the same geometry, with three terminal CO/phosphine ligands on each Ru atom, is found in the clusters of $[\text{Ru}_4\text{H}_4(\text{CO})_{12}]$ [7], $[\text{Ru}_4\text{H}_4(\text{CO})_{10}(\text{PPh}_3)_2]$ [7] and $[\text{Ru}_4\text{H}_4(\text{CO})_{11}\{\text{P}(\text{OMe})_3\}]$ [5]. Selected bond lengths and angles of **1** are summarized in Table 1. The average bond distances and bond angles of **1** are compared with those of two other clusters with Ru_4 metal core in Table 2. The clusters have almost the same Ru–Ru bond distances. The metal–carbon bond

* Corresponding author.

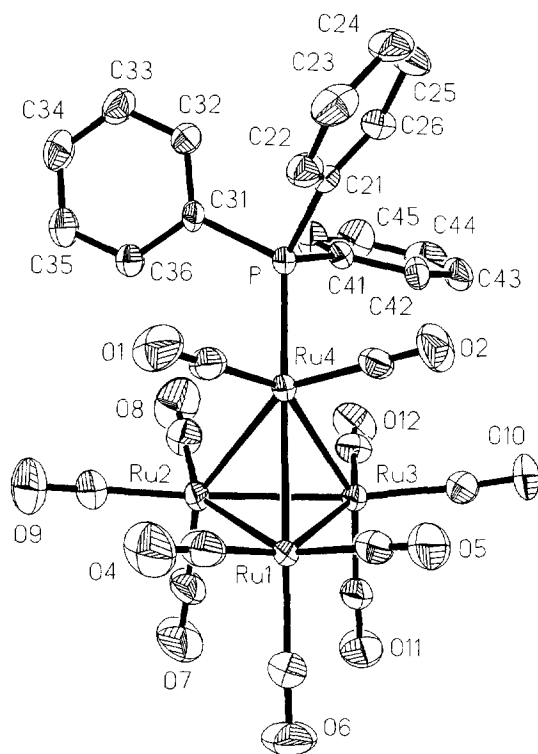


Fig. 1. The molecular structure of $[\text{Ru}_4\text{H}_4(\text{CO})_{11}(\text{PPh}_3)]$ (**1**) with the atom labelling scheme. The hydrogen atoms μ_2 -bonded to the Ru–Ru edges were not located by X-ray methods, and all other hydrogen atoms have been omitted for clarity. The thermal ellipsoids are drawn at 35% probability level.

lengths are slightly longer in **1** and $[\text{Ru}_4\text{H}_4(\text{CO})_{12}]$ than in $[\text{Ru}_4\text{H}_4(\text{CO})_{10}(\text{PPh}_3)_2]$. The room-temperature ^1H NMR spectrum of **1** exhibits one sharp hydride resonance at $\delta -17.3$ ppm, which is split by the $^2J(\text{P}-\text{H})$ coupling (4.1 Hz). This can be assigned to the $\text{Ru}(\mu_2\text{-H})\text{Ru}$ bridging hydrogen atoms, which are equivalent. The ^1H NMR spectrum of **1** has also been reported earlier [3]. The room-temperature $^{31}\text{P}\{^1\text{H}\}$ NMR spectrum of **1** shows resonance at $\delta +38.7$ ppm, which is typical of a shift to a cluster of the PPh_3 ligand.

The four cluster hydrogen atoms were not located directly, but a consideration of the orientation of the carbonyl ligands and the Ru–Ru bond lengths suggests that the edges Ru(1)–Ru(2), Ru(1)–Ru(3), Ru(2)–Ru(4) and Ru(3)–Ru(4) are bridged by the hydrogen atoms. The non-bridged Ru(1)–Ru(4) and Ru(2)–Ru(3) edges are shorter (av. 2.793 Å) than the bridged ones (av. 2.935 Å). In $[\text{Ru}_4\text{H}_4(\text{CO})_{12}]$ the corresponding Ru–Ru bond distances are 2.786 and 2.950 Å [7], in $[\text{Ru}_4\text{H}_4(\text{CO})_{10}(\text{PPh}_3)_2]$ 2.775 and 2.965 Å [8] or 2.772 and 2.966 Å [7], and in $[\text{Ru}_4\text{H}_4(\text{CO})_{11}\{\text{P}(\text{OMe})_3\}]$ 2.76 and 2.93 Å respectively [5]. The $\text{Ru}_{\text{apical}}-\text{Ru}_{\text{basal}}-\text{C}_{\text{eq}}$ angles associated with hydride-bridged Ru–Ru bonds are typically 103–105°, whereas those associated with the non-bridged bonds are much smaller, typically ca. 95°.

2.2. Spectroscopic data and solid state structure of $[\text{Ru}_{4-x}\text{Ir}_x\text{H}_{2-x}(\text{CO})_{12}(\text{PPh}_3)]$ ($x = 0$ or 1 (compounds **2** and **3**))

The structures of **2** and **3**, which crystallized together, contain one bridging carbonyl ligand, as shown by the peak at 1897 cm^{-1} in the IR spectrum. Few Ru_4 compounds with bridging carbonyl groups are known: $[\text{Ru}_4\text{H}(\text{CO})_{13}]^-$ anion (one $\mu_2\text{-CO}$) [11], $[\text{Ru}_4\text{H}_2(\text{CO})_{13}]$ (two $\mu_2\text{-CO}$) [10] and $[\text{Ru}_4\text{H}_2(\text{CO})_{12}]^{2-}$ dianion (three $\mu_2\text{-CO}$) [12].

According to the ^1H NMR spectra (broad signal at -17.8 ppm), the two hydrides of **2** are equivalent in solution at room temperature. The ^1H NMR spectra were not recorded at low temperatures. The $^{31}\text{P}\{^1\text{H}\}$ NMR spectra was recorded in CDCl_3 and showed a signal at $\delta +2.2$ ppm.

The disordered crystal structure of compound **2** in $[\text{Ru}_{3.82}\text{Ir}_{0.18}\text{H}_{1.82}(\text{CO})_{12}(\text{PPh}_3)]$ is presented in Fig. 2, together with the atom numbering scheme. The structure of **3** is identical except that one of the two hydride ligands is missing. Selected bond distances and angles of **2** (and **3**) are listed in Table 3. Refinement of the occupancy factor for the apical M atom gave the distribution 0.82 for Ru and 0.18 for Ir.

Structures **2** and **3** both have one $\text{Ru}(\mu_2\text{-CO})\text{Ru}$ bridging carbonyl. A similar core geometry with one bridging carbonyl group is found in $\text{PPN}[\text{Ru}_4\text{H}(\text{CO})_{13}]$ [11]. The hydride ligands in the structure of **2** (and **3**) were located crystallographically (see Fig. 2). As in $\text{PPN}[\text{Ru}_4\text{H}(\text{CO})_{13}]$ [11], they bridge two of the metal–metal bonds. Thus the hydrogen-bridged bonds M–Ru(2) (2.920(8) Å) and M–Ru(3) (2.949(11) Å) in **2** (and **3**) are clearly longer than the non-bridged bonds (average 2.800(9) Å). The corresponding values for the bridged and non-bridged bonds in $\text{PPN}[\text{Ru}_4\text{H}(\text{CO})_{13}]$ are 2.930(1) and 2.783(1) Å. Other important bond distances of **2** (and **3**) and $\text{PPN}[\text{Ru}_4\text{H}(\text{CO})_{13}]$ clusters are compared in Table 4.

The repulsion away from the hydrogens is also seen in the Ru–Ru– C_{eq} bond angle data. Thus in **2** (and **3**), the bond angles for the hydride-bridged metal–metal edges are $109.0(2)^\circ$, while those for the non-bridged metal–metal edge are only $93.7(3)^\circ$. The corresponding values for the $\text{PPN}[\text{Ru}_4\text{H}(\text{CO})_{13}]$ cluster are $112.4(2)$ and $89.5(3)^\circ$. The phosphine ligand is coordinated apically to the disordered M atom.

3. Experimental section

3.1. General comments

All reactions and manipulations except for chromatographic separations were carried out under nitrogen

Table 1
Selected bond lengths (Å) and angles (°) for $[\text{Ru}_4\text{H}_4(\text{CO})_{11}(\text{PPh}_3)]$ (1)

Ru(1)–Ru(2)	2.9092(13)	Ru(3)–Ru(1)	2.8991(11)
Ru(4)–Ru(1)	2.7777(10)	Ru(3)–Ru(2)	2.8083(11)
Ru(4)–Ru(2)	2.9668(12)	Ru(4)–Ru(3)	2.9654(11)
Ru(4)–P	2.354(2)	Ru(4)–C(1)	1.883(10)
Ru(4)–C(2)	1.888(10)	Ru(1)–C(4)	1.914(13)
Ru(1)–C(5)	1.936(12)	Ru(1)–C(6)	1.919(12)
Ru(2)–C(7)	1.887(11)	Ru(2)–C(8)	1.895(13)
Ru(2)–C(9)	1.939(11)	Ru(3)–C(10)	1.925(10)
Ru(3)–C(11)	1.910(11)	Ru(3)–C(12)	1.912(11)
Ru(3)–Ru(1)–Ru(2)	57.83(3)	Ru(1)–Ru(2)–Ru(4)	56.41(3)
Ru(4)–Ru(1)–Ru(2)	62.84(3)	Ru(1)–Ru(3)–Ru(4)	56.53(3)
Ru(4)–Ru(1)–Ru(3)	62.94(3)	Ru(1)–Ru(4)–Ru(2)	60.75(3)
Ru(2)–Ru(3)–Ru(4)	61.77(3)	Ru(1)–Ru(4)–Ru(3)	60.53(3)
Ru(3)–Ru(2)–Ru(4)	61.72(3)	Ru(3)–Ru(2)–Ru(1)	60.91(3)
Ru(3)–Ru(4)–Ru(2)	56.51(2)	Ru(2)–Ru(3)–Ru(1)	61.27(3)
P–Ru(4)–Ru(1)	170.96(6)	P–Ru(4)–Ru(2)	112.20(6)
P–Ru(4)–Ru(3)	111.25(6)	C(1)–Ru(4)–Ru(1)	92.1(3)
C(1)–Ru(4)–Ru(2)	100.8(3)	C(1)–Ru(4)–Ru(3)	150.0(3)
C(2)–Ru(4)–Ru(1)	94.0(3)	C(2)–Ru(4)–Ru(2)	150.3(3)
C(2)–Ru(4)–Ru(3)	98.6(3)	C(4)–Ru(1)–Ru(2)	99.5(4)
C(4)–Ru(1)–Ru(3)	152.7(4)	C(4)–Ru(1)–Ru(4)	94.3(3)
C(5)–Ru(1)–Ru(2)	154.5(3)	C(5)–Ru(1)–Ru(3)	103.9(4)
C(5)–Ru(1)–Ru(4)	93.6(3)	C(6)–Ru(1)–Ru(2)	106.8(4)
C(6)–Ru(1)–Ru(3)	105.4(4)	C(6)–Ru(1)–Ru(4)	167.1(4)
C(7)–Ru(2)–Ru(1)	100.7(4)	C(7)–Ru(2)–Ru(3)	93.7(4)
C(7)–Ru(2)–Ru(4)	151.8(4)	C(8)–Ru(2)–Ru(1)	153.2(4)
C(8)–Ru(2)–Ru(3)	95.7(4)	C(8)–Ru(2)–Ru(4)	102.4(4)
C(9)–Ru(2)–Ru(1)	104.1(4)	C(9)–Ru(2)–Ru(3)	163.0(4)
C(9)–Ru(2)–Ru(4)	104.0(4)	C(10)–Ru(3)–Ru(1)	105.8(3)
C(10)–Ru(3)–Ru(4)	102.7(3)	C(10)–Ru(3)–Ru(2)	163.3(3)
C(11)–Ru(3)–Ru(1)	96.0(3)	C(11)–Ru(3)–Ru(2)	93.9(3)
C(11)–Ru(3)–Ru(4)	149.1(3)	C(12)–Ru(3)–Ru(1)	155.2(3)
C(12)–Ru(3)–Ru(2)	94.9(3)	C(12)–Ru(3)–Ru(4)	107.7(3)
C(1)–Ru(4)–P	94.9(3)	C(2)–Ru(4)–P	90.9(3)
C(1)–Ru(4)–C(2)	95.3(5)	C(4)–Ru(1)–C(5)	91.6(6)
C(4)–Ru(1)–C(6)	95.2(5)	C(6)–Ru(1)–C(5)	94.8(5)
C(7)–Ru(2)–C(8)	93.3(6)	C(7)–Ru(2)–C(9)	97.3(5)
C(8)–Ru(2)–C(9)	96.6(5)	C(11)–Ru(3)–C(10)	98.2(4)
C(12)–Ru(3)–C(10)	96.0(4)	C(11)–Ru(3)–C(12)	92.3(5)

atmosphere using standard Schlenk techniques [14]. The products are not particularly sensitive to air, however.

Infrared spectra were recorded in *n*-hexane on a

Table 2
Important average bond distances (Å) and bond angles (°) in **1**, $[\text{Ru}_4\text{H}_4(\text{CO})_{12}]$ (4) [7] and $[\text{Ru}_4\text{H}_4(\text{CO})_{10}(\text{PPh}_3)_2]$ (5) [7]

	1	4	5
Ru–Ru (long distances)	2.935(1)	2.950(8)	2.967(2)
Ru–Ru (short distances)	2.793(1)	2.786(8)	2.772(2)
Ru–P	2.354(2)	—	2.359(4)
Ru–C ^a	1.903(1)	1.902(3)	1.830(1)
Ru–C ^b	1.928(1)	1.938(8)	1.850(2)
C–O	1.133(1)	1.131(3)	1.180(1)
Ru _{basal} –Ru _{apical} –C	114.3	114.5	113.7
Ru _{apical} –Ru _{basal} –C _{eq.}	100.8	101.1	101.2
Ru _{basal} –Ru _{basal} –C _{ax.}	99.4	100.3	100.2

^a Pseudo-*trans* to the long M–M bonds.

^b Pseudo-*trans* to the short M–M bonds.

Nicolet 20SXC FT-IR spectrometer. ¹H and ³¹P NMR spectra were measured on a Bruker AM-250 spectrometer with CDCl₃ as solvent. The ¹H NMR spectra were referenced to external TMS and the ³¹P spectra were referenced to external 85% H₃PO₄, such that shifts to higher frequencies relative to the reference are taken as positive.

3.2. Reagents

$[\text{Ir}(\text{CO})\text{Cl}(\text{PPh}_3)_2]$ (Strem) was of commercial origin and used without further purification. $[\text{Ru}_3(\text{CO})_{12}]$ was prepared by a literature method [15]. The cluster anion $[\text{Ru}_3\text{H}(\text{CO})_{11}]^-$ was prepared by a published procedure [16]. Tetrahydrofuran (THF) was dried and deoxygenated by stirring over Na/benzophenone ketyl, and freshly distilled before use. Other solvents were deoxygenated by bubbling N₂ through them.

3.3. Preparation of $[Ru_4H_4(CO)_{11}(PPh_3)]$ (1) in THF

A 100 ml Schlenk flask under nitrogen and equipped with a stirring bar and rubber septum was charged with $[Ir(CO)Cl(PPh_3)_2]$ (66 mg, 0.08 mmol) dissolved in 40 ml THF and a freshly prepared solution of $Na[Ru_3H(CO)_{11}]$ [16] (made from 201 mg, 0.31 mmol $[Ru_3(CO)_{12}]$). The solution, which immediately turned from yellow to dark red, was stirred for 1 h at room temperature. The solution was filtered, the solvent evap-

orated in vacuo, and the solid residue treated with 85% H_3PO_4 . Extraction with hexane gave a yellow solution of $[Ru_3(CO)_{12}]$. Further extraction with CH_2Cl_2 gave a red solution, which was evaporated in vacuo. The residue was chromatographed on a silica column. Elution with hexane gave a yellow band of $[Ru_3(CO)_{12}]$, which was residue from the extraction with hexane. Further elution with a hexane/dichloromethane (6:1) mixture gave two red bands which were difficult to separate, and finally elution with dichloromethane gave a fourth, red band.

Table 3

Selected bond lengths (Å) and angles (°) for $Ru_{4-x}Ir_xH_{2-x}(CO)_{12}(PPh_3)$ ($x = 0$ or 1) (2 or 3)

M–Ru(1)	2.792(9)	Ru(1)–Ru(2)	2.795(9)
M–Ru(2)	2.920(8)	Ru(1)–Ru(3)	2.806(10)
M–Ru(3)	2.949(11)	Ru(2)–Ru(3)	2.805(9)
M–P	2.354(2)	M–C(1)	1.883(7)
M–C(2)	1.907(7)	Ru(1)–C(4)	1.911(8)
Ru(1)–C(5)	1.897(8)	Ru(1)–C(6)	1.912(7)
Ru(2)–C(7)	1.909(7)	Ru(2)–C(8)	1.888(8)
Ru(2)–C(9)	1.902(7)	Ru(3)–C(10)	1.927(8)
Ru(3)–C(11)	1.889(8)	Ru(3)–C(12)	1.915(7)
Ru(1)–C(13)	2.036(7)	Ru(3)–C(13)	2.271(7)
Ru(1)–M–Ru(2)	58.54(2)	M–Ru(1)–Ru(2)	63.02(2)
Ru(1)–M–Ru(3)	58.44(2)	M–Ru(1)–Ru(3)	63.58(2)
Ru(2)–M–Ru(3)	57.09(2)	Ru(1)–Ru(2)–M	58.44(2)
Ru(1)–Ru(2)–Ru(3)	60.14(3)	Ru(3)–Ru(2)–M	61.98(2)
Ru(2)–Ru(1)–Ru(3)	60.10(2)	Ru(2)–Ru(3)–M	60.94(2)
Ru(2)–Ru(3)–Ru(1)	59.76(2)	Ru(1)–Ru(3)–M	57.98(2)
P–M–Ru(1)	168.17(4)	P–M–Ru(2)	116.19(5)
P–M–Ru(3)	109.74(5)	C(1)–M–Ru(1)	93.0(2)
C(1)–M–Ru(2)	94.6(2)	C(1)–M–Ru(3)	146.6(2)
C(2)–M–Ru(1)	89.5(2)	C(2)–M–Ru(2)	147.3(2)
C(2)–M–Ru(3)	102.3(2)	C(4)–Ru(1)–M	94.5(3)
C(4)–Ru(1)–Ru(2)	67.8(2)	C(4)–Ru(1)–Ru(3)	127.9(2)
C(5)–Ru(1)–M	92.8(3)	C(5)–Ru(1)–Ru(2)	146.3(3)
C(5)–Ru(1)–Ru(3)	132.0(2)	C(6)–Ru(1)–M	166.9(2)
C(6)–Ru(1)–Ru(2)	108.7(2)	C(6)–Ru(1)–Ru(3)	103.7(2)
C(7)–Ru(2)–M	143.2(2)	C(7)–Ru(2)–Ru(1)	86.9(2)
C(7)–Ru(2)–Ru(3)	91.5(2)	C(8)–Ru(2)–M	115.0(2)
C(8)–Ru(2)–Ru(1)	159.5(2)	C(8)–Ru(2)–Ru(3)	99.4(2)
C(9)–Ru(2)–M	105.0(2)	C(9)–Ru(2)–Ru(1)	110.2(2)
C(9)–Ru(2)–Ru(3)	166.3(2)	C(10)–Ru(3)–M	113.3(3)
C(10)–Ru(3)–Ru(1)	123.3(3)	C(10)–Ru(3)–Ru(2)	171.8(3)
C(11)–Ru(3)–M	146.5(2)	C(11)–Ru(3)–Ru(1)	90.9(2)
C(11)–Ru(3)–Ru(2)	94.0(2)	C(12)–Ru(3)–M	102.5(2)
C(12)–Ru(3)–Ru(1)	141.6(2)	C(12)–Ru(3)–Ru(2)	81.9(2)
C(13)–Ru(1)–M	80.5(2)	C(13)–Ru(3)–M	73.5(2)
C(13)–Ru(1)–Ru(2)	112.6(2)	C(13)–Ru(1)–Ru(3)	53.1(2)
C(13)–Ru(3)–Ru(1)	45.8(2)	C(13)–Ru(3)–Ru(2)	105.1(2)
C(1)–M–P	98.2(2)	C(2)–M–P	93.8(2)
C(1)–M–C(2)	93.5(3)	C(5)–Ru(1)–C(4)	92.9(4)
C(6)–Ru(1)–C(4)	91.2(3)	C(5)–Ru(1)–C(6)	98.7(4)
C(8)–Ru(2)–C(7)	93.0(3)	C(9)–Ru(2)–C(7)	97.9(3)
C(9)–Ru(2)–C(8)	90.1(3)	C(11)–Ru(3)–C(10)	93.5(4)
C(12)–Ru(3)–C(10)	94.2(3)	C(11)–Ru(3)–C(12)	94.8(3)
C(4)–Ru(1)–C(13)	173.7(3)	C(5)–Ru(1)–C(13)	83.6(3)
C(6)–Ru(1)–C(13)	94.5(3)	C(10)–Ru(3)–C(13)	77.6(3)
C(11)–Ru(3)–C(13)	94.3(3)	C(12)–Ru(3)–C(13)	168.1(3)
Ru(1)–C(13)–Ru(3)	81.1(3)		

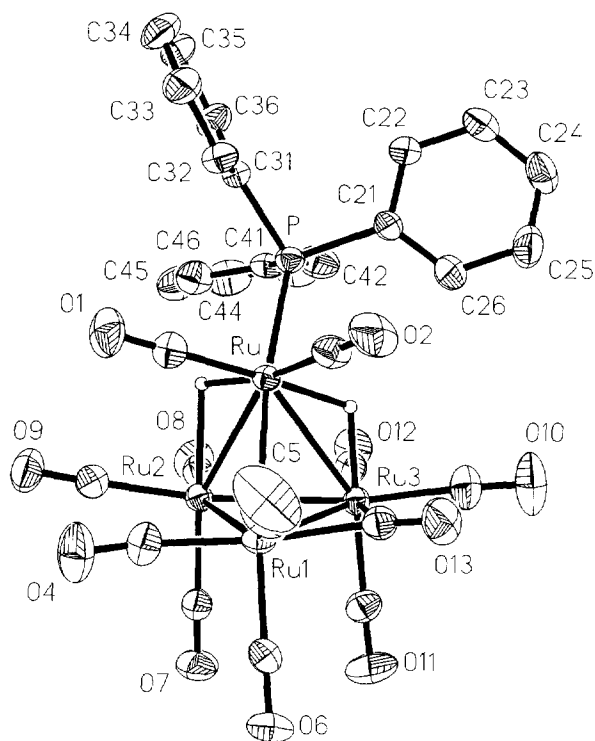


Fig. 2. The molecular structure of $[\text{Ru}_{4-x}\text{Ir}_x\text{H}_{2-x}(\text{CO})_{12}(\text{PPh}_3)]$ ($x = 0$ and 1 (compounds **2** and **3**)) with the atom labelling scheme. The thermal ellipsoids are drawn at 35% probability level. The hydrogen atoms, except those bound to two metal atoms, have been omitted for clarity.

The mixture of the second and third bands was refluxed for 2 h in hexane under hydrogen atmosphere. After the reaction the solvent was evaporated in vacuo and the residue chromatographed by TLC. Elution with a hexane/dichloromethane (4:1) mixture gave seven bands, of which the first was identified as $[\text{Ru}_3(\text{CO})_{12}]$. The second band (yield < 10%) was structurally characterized as **1** by X-ray diffraction of the yellow crystals obtained upon crystallization from CH_2Cl_2 /hexane mixture. Analysis of the third and fourth bands is in progress [13]. The remaining three bands (5–7) were

Table 4
Important average bond distances (Å) in $[\text{Ru}_{3.82}\text{Ir}_{0.18}\text{H}_{1.82}(\text{CO})_{12}(\text{PPh}_3)]$ **2** (and **3**) and $\text{PPN}[\text{Ru}_4\text{H}(\text{CO})_{13}]$ (**6**) [11]

	2 (and 3)	6
Ru–Ru (long distances)	2.935(5)	2.930(1)
Ru–Ru (short distances)	2.800(9)	2.783(1)
Ru–P	2.354(2)	—
Ru–C ^a	1.897(7)	1.902(8)
Ru–C ^b	1.907(9)	1.889(8)
Ru–C _{bridged}	2.154(7)	2.137(7)
C–O	1.136(8)	1.140(8)
C _{bridged} –O _{bridged}	1.167(9)	1.165(7)

^a Pseudo-*trans* to the long M–M bonds.

^b Pseudo-*trans* to the short M–M bonds.

not fully identified. IR spectrum of **1** (hexane, cm^{-1}): ν_{CO} 2095m, 2087w, 2068vs, 2059s, 2050m, 2028vs, 2016m, 2009m, 1998w, 1991w and 1969w. ^1H NMR spectrum (CDCl_3 , 293 K): δ 7.47 (s, C_6H_5), 7.46 (s, C_6H_5), 7.44 (s, C_6H_5) and -17.3 ppm (d, Ru–H–Ru). $^{31}\text{P}\{^1\text{H}\}$ NMR spectrum (CDCl_3 , 293 K): δ +38.7 ppm.

3.4. Preparation of $[\text{Ru}_4\text{H}_2(\text{CO})_{12}(\text{PPh}_3)]$ (**2**) in THF

A Schlenk flask was charged with $[\text{Ir}(\text{CO})\text{Cl}(\text{PPh}_3)_2]$ (235 mg, 0.30 mmol) and 30 ml of THF. To the homogeneous yellow mixture was added a freshly prepared and filtered solution of $\text{Na}[\text{Ru}_3\text{H}(\text{CO})_{11}]$ [16] (made from 227 mg, 0.36 mmol $[\text{Ru}_3(\text{CO})_{12}]$) in THF (30 ml). The reaction mixture, which immediately turned a deep reddish brown, was stirred for 1 h at ambient temperature. The solvent was evaporated in vacuo and the resulting solid extracted with hexane. The hexane solution was evaporated to dryness, giving $[\text{Ru}_3(\text{CO})_{12}]$. Further extraction with CH_2Cl_2 gave a red solution, which was evaporated in vacuo. The residue was chromatographed on a silica column. A first elution with hexane gave a broad yellow band of $[\text{Ru}_3(\text{CO})_{12}]$, which was a residue from the extraction with hexane. Further elution with a hexane/dichloromethane (6:1) mixture gave two yellowish brown bands (**2** and **3**), and finally elution with dichloromethane gave red and yellow bands (**4** and **5**). A preliminary IR and ^1H NMR spectroscopic investigation of these last four bands suggested the presence of mixed-metal clusters.

The third band was repurified by TLC. After a few minutes the TLC plate indicated the presence of three fractions, which were eluted with a hexane/dichloromethane (5:1) mixture. Compound $[\text{Ru}_4\text{H}_2(\text{CO})_{12}(\text{PPh}_3)]$ (**2** (and **3**)) (yield < 5%) was collected as the second, orange fraction and identified by IR and ^1H and ^{31}P NMR spectroscopic data and a complete single crystal X-ray diffraction study. Attempts to separate compound **2** and **3** failed. Characterization of the other fractions is in progress [13].

Dark reddish brown crystals of **2** (and **3**) were grown by slow evaporation from saturated CH_2Cl_2 /hexane mixture. IR (hexane, cm^{-1}): ν_{CO} 2092w, 2089sh, 2067w, 2054s, 2050vs, 2039m, 2029s, 2013w, 2003w, 1998w, 1989w, 1981w and 1897m. ^1H NMR spectrum (CDCl_3 , 263 K): δ 7.47 (br, C_6H_5) and -17.8 ppm (br, Ru–H–Ru). $^{31}\text{P}\{^1\text{H}\}$ NMR spectrum (CDCl_3 , 293 K): δ +2.2 ppm.

3.5. Data collection and structure analysis of **1** and **2** (and **3**)

Crystals were mounted on a glass fibre. Axial photographs indicated the triclinic crystal system for **1** and the monoclinic crystal system for **2** (and **3**). Details of crystal parameters, data collection parameters, and re-

Table 5
Crystallographic data for compounds **1** and **2** (and **3**)

	1	2 (and 3)
Formula	Ru ₄ C ₂₉ H ₁₉ O ₁₁ P	Ru _{3.82} Ir _{0.18} C ₃₀ H _{16.82} O ₁₂ P
Formula weight	978.73	1020.85
Crystal system	Triclinic	Monoclinic
Space group	<i>P</i> $\bar{1}$	<i>P</i> 2 ₁ / <i>c</i>
<i>a</i> (Å)	8.971(2)	12.820(3)
<i>b</i> (Å)	9.361(2)	15.387(4)
<i>c</i> (Å)	21.741(4)	17.787(5)
α (°)	88.53(1)	
β (°)	87.84(2)	106.74(2)
γ (°)	64.19(1)	
<i>V</i> (Å ³)	1642.4(6)	3360.0(2)
<i>Z</i>	2	4
<i>D</i> _{calc} (g cm ⁻³)	1.98	2.02
Crystal dimensions (mm ³)	0.15 × 0.25 × 0.40	0.40 × 0.40 × 0.40
Monochromator	graphite	graphite
Radiation	Mo K α	Mo K α
μ (Mo K α) (cm ⁻¹)	18.7	25.0
2 θ limits (°)	5–55	5–55
No. of unique data	7570	7750
<i>I</i> > 2 σ (<i>I</i>)	5208	5758
No. of parameters	406	431
<i>R</i> [<i>I</i> > 2 σ (<i>I</i>)] ^a	0.062	0.048
<i>wR</i> (<i>F</i> ²) [all data] ^b	0.172 ^c	0.135 ^d
Goodness of fit	1.062	1.082

^a $R = \sum ||F_o| - |F_c|| / \sum |F_o|$.

^b $w = 1 / [\sigma^2(F_o^2) + (aP)^2 + bP]$; $P = [(F_o^2) + 2F_c^2] / 3$.

^c $a = 0.0875$ and $b = 4.20$.

^d $a = 0.0594$ and $b = 2.40$.

finer data for **1** and **2** (and **3**) are summarized in Table 5. Parameters were obtained by carefully measuring the setting angles of 25 reflections on a Nicolet R3m diffractometer. Intensities were collected by the ω scan mode using graphite monochromated Mo K α radiation ($\lambda = 0.71073$ Å). The scan widths were 1.0° (**1**) and 0.8° (**2/3**) from K $\alpha_{1,2}$ and the scan rate varied from 4.9 to 29.3° 2 θ min⁻¹ depending on the intensity of the reflection. Intensities were corrected for background, polarization and Lorentz factors. Empirical absorption correction was made for **1** from ψ -scan data, the maximum and minimum transmission factors being 0.425 and 0.322 respectively. The intensities of three check reflections were monitored after every 97 reflections and were found to be stable. A total of 7570 reflections for **1** and 7750 for **2** (and **3**) were collected.

The metal atom positions were solved by direct methods with use of the SHELXTL program package [17]. All remaining non-hydrogen atoms were located by the usual combination of full-matrix least-squares refinement and difference electron density syntheses using SHELXL-93 [18]. Non-hydrogen atoms were refined anisotropically. Phenyl protons were placed at idealized positions (C–H = 0.93 Å, $1.2 \times U_{iso}$ Å² of parent atom). Hydride ligands were located for **2** (and **3**) from a difference Fourier map and refined with fixed isotropic

temperature factor ($U = 0.08$ Å²). For compound **2** (and **3**), the occupancy factor for the atom M involved in substitutional disorder is 0.82 for Ru and 0.18 for Ir.

4. Supplementary material available

A complete list of bond lengths and angles, and tables of thermal parameters and hydrogen atom coordinates, have been deposited at the Cambridge Crystallographic Data Centre.

References

- [1] B.F.G. Johnson, R.D. Johnston, J. Lewis and B.H. Robinson, *J. Chem. Soc., Chem. Commun.*, (1966) 851.
- [2] J.W.S. Jamieson, J.V. Kingston and G. Wilkinson, *J. Chem. Soc., Chem. Commun.*, (1966) 569.
- [3] F. Piacenti, M. Bianchi, P. Frediani and E. Benedetti, *Inorg. Chem.*, 10 (1971) 2759.
- [4] S.A.R. Knox and H.D. Kaesz, *J. Am. Chem. Soc.*, 93 (1971) 4594.
- [5] R.D. Wilson and R. Bau, *J. Am. Chem. Soc.*, 98 (1976) 4687.
- [6] B.F.G. Johnson, R.D. Johnston, J. Lewis, B.H. Robinson and G. Wilkinson, *J. Chem. Soc. A*, (1968) 2856.
- [7] R.D. Wilson, S.M. Wu, R.A. Love and R. Bau, *Inorg. Chem.*, 17 (1978) 1271.

- [8] K. Sasvari, P. Main, F.H. Cano, M. Martinez-Ripoll and P. Frediani, *Acta Crystallogr.*, B35 (1979) 87.
- [9] B.F.G. Johnson, R.D. Johnston and J. Lewis, *J. Chem. Soc. A*, (1968) 2865.
- [10] D.B.W. Yawney and R.J. Doedens, *Inorg. Chem.*, 11 (1972) 838.
- [11] J.A. Jensen, D.E. Fjare and W.L. Gladfelter, *Inorg. Chem.*, 22 (1983) 1250.
- [12] K.E. Inkrott and S.G. Shore, *J. Am. Chem. Soc.*, 100 (1978) 3954.
- [13] A.U. Härkönen, M. Ahlgrén, T.A. Pakkanen and J. Pursiainen, *Organometallics*, in press.
- [14] D.F. Shriver and M.A. Drezdson, *The Manipulation of Air-Sensitive Compounds*, Wiley, New York, 2nd edn., 1986.
- [15] C.R. Eady, P.F. Jackson, B.F.G. Johnson, J. Lewis, M. Malatesa, M. McPartlin and W.J.H. Nelson, *J. Chem. Soc., Dalton Trans.*, (1980) 383.
- [16] B.F.G. Johnson, J. Lewis, P.R. Raithby and G. Süß, *J. Chem. Soc., Dalton Trans.*, (1978) 1356.
- [17] G.M. Sheldrick, SHELXTL-PLUS, Release 4.11/v, Siemens Analytical X-ray Instruments Inc., Madison, WI, 1990.
- [18] G.M. Sheldrick, SHELXL-93, Program for the Refinement of Crystal Structures, University of Göttingen, Germany, 1993.